

CORE SHAPES AND ORIENTATIONS OF CORE-SÉRSIC GALAXIES

BILLIGN T. DULLO¹, ALISTER W. GRAHAM¹

¹ Centre for Astrophysics and Supercomputing, Swinburne University of Technology, Hawthorn, Victoria 3122, Australia;
Bdullo@astro.swin.edu.au

Draft version June 17, 2021

ABSTRACT

The inner and outer shapes and orientations of core-Sérsic galaxies may hold important clues to their formation and evolution. We have therefore measured the central and outer ellipticities and position angles for a sample of 24 core-Sérsic galaxies using archival *HST* images and data. By selecting galaxies with core-Sérsic break radii R_b —a measure of the size of their partially depleted core—that are $\gtrsim 0''.2$, we find that the ellipticities and position angles are quite robust against *HST* seeing. For the bulk of the galaxies, there is a good agreement between the ellipticities and position angles at the break radii and the average outer ellipticities and position angles determined over $R_e/2 < R < R_e$, where R_e is the spheroids’ effective half light radius. However there are some interesting differences. We find a median “inner” ellipticity at R_b of $\epsilon_{\text{med}} = 0.13 \pm 0.01$, rounder than the median ellipticity of the “outer” regions $\epsilon_{\text{med}} = 0.20 \pm 0.01$, which is thought to reflect the influence of the central supermassive black hole at small radii. In addition, for the first time we find a trend, albeit weak (2σ significance), such that galaxies with larger (stellar deficit)-to-(supermassive black hole) mass ratios—thought to be a measure of the number of major dry merger events—tend to have rounder inner and outer isophotes, suggesting a connection between the galaxy shapes and their merger histories. We show that this finding is not simply reflecting the well known result that more luminous galaxies are rounder, but it is no doubt related.

Subject headings: galaxies: elliptical and lenticular, cD — galaxies: fundamental parameter — galaxies: nuclei — galaxies: photometry — galaxies: structure

1. INTRODUCTION

In the hierarchical structure formation model, massive early-type galaxies are believed to be formed via galaxy mergers (e.g., Toomre & Toomre 1972; Schweizer 1982; Barnes 1988; Kauffmann, White & Guiderdoni 1993). The most favored core-Sérsic galaxy formation scenario predicts the creation of their partially depleted cores by the action of coalescing supermassive black hole (SMBH) binaries within the merged remnant of their gas-poor progenitors. The energy which is transferred from the SMBH binary’s orbital decay causes the slingshot ejection of the inner stars, creating the stellar light deficits of core-Sérsic galaxies (e.g., Begelman et al. 1980; Ebisuzaki et al. 1991; Milosavljević & Merritt 2001; Merritt 2006). This three-body scattering process preferentially removes stars on radial (eccentric) orbits, resulting in tangentially biased (circular) orbits in the core region of core-Sérsic galaxies, and excess levels of radial orbits beyond the core (e.g., Quinlan & Hernquist 1997; Milosavljević & Merritt 2001; Gebhardt et al. 2003). Thomas et al. (2014) have recently found these kinematical signatures in six core-Sérsic galaxies. It, therefore, seems reasonable that the inner isophotal shape, orientation (position angle) and radial light distribution of a core-Sérsic galaxy may be connected to each other and to the details of the physical processes that built the galaxy at large. For instance, does the orientation of the core still reflect the orbital plane of the merging SMBHs, and does that also reflect the orbital alignment of the pre-merged galaxies and the final outer/global isophotal shape of the wedded galaxy pair? Such questions are the main motivation for this work.

“Core-Sérsic” galaxies have central light deficits relative to the (steeper) inward extrapolation of their spheroids’ (i.e., elliptical galaxies’ or bulges’) outer Sérsic profile (Graham et al. 2003), while “core” galaxies with an inner slope $\gamma < 0.3$ (Lauer et al. 1995) do not necessarily have deficits relative to the outer Sérsic profile. The Nuker model break radii are typically 2 – 3 times larger than the core-Sérsic model break radii (e.g., Trujillo et al. 2004); i.e., they are somewhat outside of the main depleted core and therefore not an ideal location to measure the core’s ellipticity and position angle. However, the smaller radius where the negative, logarithmic slope of the projected light profile equals 0.5 can be derived from the Nuker model parameters (Carollo et al. 1997; Rest et al. 2001) and matches very well with the core-Sérsic break radius (Dullo & Graham 2012). However, Dullo & Graham (2012) found that $\sim 18\%$ of “cores” according to the Nuker model are not depleted cores according to the core-Sérsic model and as such, application of the core-Sérsic model is still required if one wishes to identify galaxies with partially depleted cores rather than simply flattish inner (non-depleted) Sérsic light profiles. Graham (2004) asked whether the ellipticity (and position angle) at the break radii of actual partially depleted cores in core-Sérsic galaxies agrees and aligns with the outer spheroids’ ellipticity (and position angle). With a sufficiently large ($N=24$) sample we can now start to probe this question.

Previous works on the evolution of triaxial galaxies had indicated that a central supermassive black hole would destroy the inner box orbits leaving a rounder or nearly spherical core (e.g., Norman, May, & van Albada 1985;

Gerhard & Binney 1985; Merritt & Quinlan 1998; Merritt 2000; Holley-Bockelmann et al. 2002; Merritt & Poon 2004), while the outer parts of core-Sérsic spheroids are thought to be built, shaped and oriented by dissipationless, major galaxy merging and the ensuing strong violent relaxation and phase mixing (e.g., van Albada 1982; McGlynn 1984; Burkert et al. 2008; Hopkins et al. 2009). In addition, the change in the shapes and orientations of the isophotes at large radii may arise from the effect of tidal encounters with nearby massive companions (Nieto & Bender 1989; Hao et al. 2006), and the presence of isophotal twisting in galaxies are also commonly associated with triaxiality, bars, disks or dust lanes (e.g., Nieto et al. 1992). In this paper, we investigate the radial changes of the shapes and orientations of core-Sérsic galaxies, and the implications for their formation and evolution. We note that core-Sérsic galaxies are not confined to elliptical galaxies. Lenticular disc galaxies, i.e., “fast rotators”, are also known to contain partially-depleted cores relative to their bulge’s main Sérsic profile (Dullo & Graham 2013; Krajnović et al. 2013). While these discs may be associated with the galaxy’s previous merger event (e.g., Naab & Burkert 2003), they may have been subsequently accreted from cold gas flows, possibly fed along streams of a fixed orientation (Pichon et al. 2011). In what follows we use the shapes of the bulge, or bulge-dominated, region of the galaxies.

In Section 2 we describe our data selection, and isophotal profile extraction techniques. The measurements of the inner and outer ellipticities and orientations of the galaxies are presented in Sections 3 and 4, respectively. Section 5 discusses the implications of these results in the context of core-Sérsic galaxy formation and evolution. We also compare our study with previous works. Our main conclusions are summarized in Section 6.

2. GALAXY SAMPLE AND PROFILES

We have used the IRAF task ELLIPSE (Jedrzejewski 1987) to extract ellipticity and position angle profiles from *HST* WFPC2 and ACS images of a sample of 24 nearby (~ 10 -100 Mpc) core-Sérsic galaxies with $M_V \lesssim -20.7$ mag presented in Dullo & Graham (2014). These images were retrieved from the Hubble Legacy Archive¹. All the 24 galaxies in our sample have partially depleted cores relative to their outer Sérsic profile (see Table 1). They have come from an initial sample of 39 galaxies (Lauer et al. 2005) with shallow inner profile slopes, but not necessarily depleted cores (see Dullo & Graham 2012, 2013). Excluding seven Sérsic galaxies (which do not have depleted cores) and one dusty galaxy, in Dullo & Graham (2014) we studied 31 of these core-Sérsic galaxies. Here, we excluded seven core-Sérsic galaxies from the Dullo & Graham (2014) sample. Specifically, NGC 1700, NGC 3640 and NGC 7785 because they have questionably small cores ($R_b \lesssim 0''.04$, Dullo & Graham 2014), and as such the ellipticity and position angle measurements at their break radii cannot be trusted. For NGC 3706, NGC 4073, NGC 4406 and NGC 6876, Lauer et al. (2005) did not publish the inner ($R \lesssim 1''$) isophote ellipticity and position angle profiles because their ELLIPSE fits were unstable for these inner isophotes.

To check on the influence of the *HST*’s Point Spread

¹ <http://hla.stsci.edu>

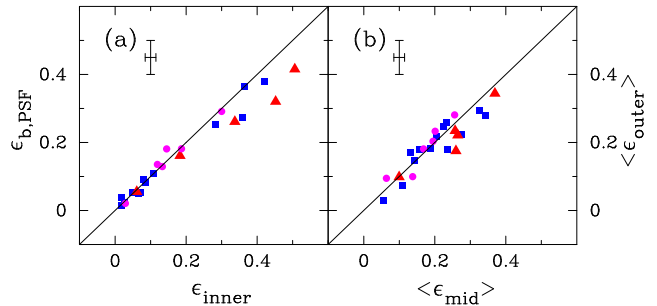


FIG. 1.— Panel (a): PSF-affected ellipticity measured at the core-Sérsic break radius ($\epsilon_{b,\text{PSF}}$) plotted against the Lauer et al. (2005) PSF-deconvolved ellipticity at the core-Sérsic break radius (ϵ_{inner}). Panel (b): average ellipticity determined at $R > R_e$ ($\langle \epsilon_{\text{outer}} \rangle$) versus average ellipticity measured between $R_e/2$ and R_e ($\langle \epsilon_{\text{mid}} \rangle$). Circles and squares represent core-Sérsic elliptical galaxies with and without additional nuclear light components, respectively. Triangles designate core-Sérsic lenticular galaxies.

Function (PSF), we have additionally used the inner ($R \lesssim 3''$) Lauer et al. (2005) PSF-deconvolved ellipticities and position angles². Details of our data reduction and isophotal parameter extraction procedures are discussed in Dullo & Graham (2013).

For comparison, we (Bonfini et al. 2014, in prep.) also derived ellipticity and position angle profiles by fitting PSF-convolved 2D core-Sérsic models to the galaxy images using GALFIT (Peng et al. 2002; Bonfini 2014). In general, our ellipticities and position angles determined from the 1D ELLIPSE fits agree reasonably well with i) the results based on GALFIT (see also Floyd et al. 2008 for similar conclusions) and ii) those from Lauer et al. (2005) for $R \gtrsim 0''.2$ and out to their outer most radii of $\approx 10 - 15''$. Here we use profiles out to $\approx 100''$, typically extending beyond the galaxies half light radii. In this work, we use the ellipticities and position angles from the ELLIPSE fits because GALFIT fits PSF-convolved elliptical core-Sérsic models with fixed (i.e., singular) ellipticities and position angles to the galaxy images. However, the shapes and orientations of galaxies can of course change with radius (e.g., di Tullio 1979; Kent 1984; Zaritsky & Lo 1986, Bender et al. 1988; Cappacioli et al. 1988). Table 1 presents the morphological classification, core-Sérsic break radii, spheroids’ effective half light radii, ellipticities and position angles for our sample galaxies³.

3. ELLIPTICITIES

3.1. Assessment of the ellipticity measurements

In Fig. 1a, we test the effect of the *HST* WFPC2/ACS PSF by comparing our ellipticities determined from the ELLIPSE fits with the Lauer et al. (2005) PSF-deconvolved ellipticities, both measured (by us) at the core-Sérsic break radius. The *HST*’s WFPC2/ACS seeing has a full width at half-maximum, FWHM $\approx 0''.1$. In general, PSF smearing biases inner galaxy isophotes towards rounder ellipticities (e.g., Rest et al. 2001; Rahman & Shandarin 2003; Holden et al. 2009). Simulations by Holden et al. (2009), for example, showed that *HST*’s PSF causes the apparent ellipticities of high redshift ($z > 0.3$) early-type galaxies to be underestimated.

² http://www.noao.edu/noao/staff/lauer/wfpc2_profs/

³ The average values were derived using a logarithmic sampling of the radius.

Nonetheless, the “break ellipticities⁴” from our ELLIPSE fit ($\epsilon_{b,\text{PSF}}$) and those from Lauer et al. (2005), ϵ_{inner} , agree within the errors, indicating minimum PSF contamination at our galaxy sample’s break radii, which are all $> 0''.2$.

As can be seen in Fig. 1a, there is a systematic tendency for the ellipticity of the most elliptical cores to be slightly under-estimated from the ELLIPSE fits. This is likely due to seeing. Throughout this paper we use the Lauer et al. (2005) PSF-deconvolved ellipticity profile sampled at our core-Sérsic break radius (ϵ_{inner}) and the average spheroid ellipticity measured by us using our ELLIPSE data over the interval $R_e/2$ to R_e (denoted $\langle\epsilon_{\text{mid}}\rangle$) as the spheroid’s representative inner and mid-range ellipticities, respectively (Table 1). Note that our average ellipticities and position angles (Table 1) are not luminosity weighted.

Six of our 24 galaxies (NGC 0741, NGC 4278, NGC 4365, N4472, NGC 4552 and NGC 5419) have additional nuclear light components (Dullo & Graham 2012). For four of these nucleated galaxies (i.e., except for NGC 4365 and NGC 5419), both ϵ_{inner} and $\langle\epsilon_{\text{mid}}\rangle$ are lower than $\lesssim 0.20$ and their central light excess is due to a point-source AGN (Dullo & Graham 2012, their Section 8). For NGC 5419, Lena et al. (2014) noted that it has a double nucleus (see also Lauer et al. 2005). They found that the galaxy photocenter is displaced by ~ 7.5 pc and 62 pc (i.e., $\lesssim 0.15R_{b,\text{N5419}}$) from these nuclei. Thus, the double nucleus is unlikely to affect our measurement of the ellipticity at this galaxy’s core-Sérsic break radius $R_{b,\text{N5419}}=416$ pc (Dullo & Graham 2014). The elliptical galaxy NGC 4365, with $\epsilon_{\text{inner}} \sim 0.30$ and $\langle\epsilon_{\text{mid}}\rangle \sim 0.26$, has an elongated nuclear stellar cluster (e.g., Carollo et al. 1997; Lauer et al. 2005; Côté et al. 2006; Dullo & Graham 2012). Carollo et al. (1997) noted that this nucleus extends from $1''$ to $3''$, compared to this galaxy’s core-Sérsic break radius $R_{b,\text{N4365}}=1''.21$ (Dullo & Graham 2014). Therefore, our measurements of ϵ_{inner} and $\langle\epsilon_{\text{mid}}\rangle$ for NGC 4365 are likely to be influenced by its nucleus.

In order to assess the stability of the outer ellipticities, in Fig. 1b, we compare $\langle\epsilon_{\text{mid}}\rangle$ with the average spheroid ellipticity between R_e and the outermost ($R \approx 100''$) data point ($\langle\epsilon_{\text{outer}}\rangle$). Overall, Fig. 1b shows that the spheroid’s ellipticity profile remains stable over $R_e/2 \lesssim R \lesssim 100''$. Due, however, to potential tidal effects at large radii, or not fully relaxed outer regions, and the increasing dominance of disk light in the lenticular galaxies, we have elected to use $\langle\epsilon_{\text{mid}}\rangle$ to represent the spheroid outside of its core region.

An additional interesting test of our adopted ellipticities is the comparison to published inner and outer ellipticities by Ryden et al. (2001, their Table 1) and Lauer et al. (2005, their Table 5). Figs. 2a and 2b show that our ellipticity measurements generally agree well with the differently measured ellipticities from those two works. However, for NGC 4382 and NGC 5813, the inner ellipticity at the core-Sérsic break radius disagrees with the Lauer et al. (2005) average luminosity weighted ellipticities inside the Nuker break radius. These two galaxies

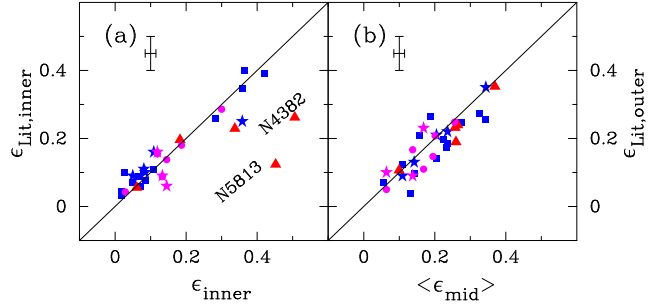


FIG. 2.— Panel (a): our break radius ellipticity ϵ_{inner} plotted against various inner ellipticities from the literature, $\epsilon_{\text{lit,inner}}$: the Ryden et al. (2001, their Table 1) inner ($R = R_e/16$) ellipticity for 10 core-Sérsic galaxies (filled stars), and inner luminosity-weighted, average ellipticity taken from Lauer et al. (2005, their Table 5). Panel (b): our average ellipticity between $R_e/2$ and R_e ($\langle\epsilon_{\text{mid}}\rangle$) plotted against outer ellipticities from the literature, $\epsilon_{\text{lit,outer}}$: the Ryden et al. (2001, their Table 1) outer ($R = R_e$, Ryden et al. 2001) ellipticity (filled stars), and outer ellipticities from Lauer et al. (2005, their Table 5). Symbols have the same meaning as in Fig. 1.

have PSF-deconvolved ellipticity profiles which steadily decrease from ~ 0.5 at R_b to ~ 0.1 at the galaxies’ innermost regions ($R \sim 0''.02$). While this might be due to the PSF, Rest et al. (2001) and Lauer et al. (1998; 2005) argued that the deconvolution process can robustly remove the effect of the PSF. These gradients are therefore thought to be real.

3.2. Inner and outer core-Sérsic galaxy ellipticities

Fig. 3 plots the Lauer et al. (2005) PSF-deconvolved ellipticity at our core-Sérsic break radius (ϵ_{inner}) against the average ellipticity between $R_e/2$ and R_e ($\langle\epsilon_{\text{mid}}\rangle$) for 24 core-Sérsic spheroids. The solid horizontal lines connect the lowest and the highest ellipticity values between $R_e/2$ and R_e for the individual galaxies. At first glance there is no obvious correlation between the core ellipticity (ϵ_{inner}) and spheroid ellipticity ($\langle\epsilon_{\text{mid}}\rangle$), the Pearson correlation coefficient for this distribution is $r \approx 0.13$ with the corresponding probability of happening by chance $P(r) \approx 50\%$. However, removing three outliers (NGC 5813, NGC 5982 and NGC 6849) reveals a general trend of broadly similar ellipticities.

The $\epsilon_{\text{inner}} - \langle\epsilon_{\text{mid}}\rangle$ correlation becomes even more pronounced when we include the Ryden et al. (2001, their Table 1) inner ϵ ($R = R_e/16$) and outer ϵ ($R = R_e$) ellipticities for 16 additional bright galaxies which were classified as “core” galaxies using the Nuker model (Fig. 3, open crosses). However, the caveats are that i) these “core” galaxies may not be equivalent to core-Sérsic galaxies (Dullo & Graham 2012) and ii) the Ryden et al. innermost fiducial radius $R_e/16$ is about a factor of three larger than the core-Sérsic break radius $R_b \approx 0.02R_e$ (Côté et al. 2007). Nonetheless, comparing the inner and outer isophote ellipticities of early-type galaxies, Ryden et al. (2001, their Fig. 1) and Lauer et al. (2005, their Fig. 5) highlighted the absence of a systematic variation of the spheroid ellipticity with radius, a result largely confirmed here.

In Fig. 4, as a further assessment of the influence of the PSF, we explore $\Delta\epsilon (= \epsilon_{\text{inner}} - \langle\epsilon_{\text{mid}}\rangle)$ as a function of the break radii and find no trend. That is, there is not a trend for galaxies with small cores to have rounder cores (a potential artifact of seeing).

⁴ Throughout this paper, the terms “break ellipticity” and “break position angle” refer to the measurements of the ellipticity and position angle at the core-Sérsic break radius (Table 1).

TABLE 1
 CORE-SÉRSIC GALAXY DATA.

Galaxy	Type	R_b (arcsec)	R_e (arcsec)	$\epsilon_{b,\text{PSF}}$	ϵ_{inner}	$\langle\epsilon_{\text{mid}}\rangle$	$\langle\epsilon_{\text{outer}}\rangle$	P.A. $_{b,\text{PSF}}$ (deg)	P.A. $_{\text{inner}}$ (deg)	$\langle\text{P.A.}_{\text{mid}}\rangle$ (deg)	$\langle\text{P.A.}_{\text{outer}}\rangle$ (deg)
(1)	(2)	(3)	(4)	(5)	(6)	(7)	(8)	(9)	(10)	(11)	(12)
NGC 0507	S0	0.33	5.3	0.261	0.337	0.260	0.176	10.8	20.3	10.6	14.8
NGC 0584	E ^d	0.21	112.5	0.272	0.358	0.344	0.279	60.0	59.2	68.7	58.6
NGC 0741	E	0.76	53.0	0.021	0.029	0.195	0.204	52.2	125.9	89.9	88.7
NGC 1016	E	0.48	41.7	0.025	0.025	0.056	0.030	80.0	40.1	34.7	9.6
NGC 1399	E	2.30	36.6	0.082	0.086	0.109	0.075	112.4	112.1	110.0	95.7
NGC 2300	S0	0.53	7.7	0.162	0.183	0.257	0.235	78.6	78.6	74.5	73.9
NGC 3379	E	1.21	50.2	0.092	0.081	0.142	0.147	61.1	70.8	66.5	64.5
NGC 3608	E	0.23	68.7	0.110	0.109	0.236	0.179	72.9	65.0	82.1	92.3
NGC 3842	E	0.72	102.4	0.014	0.017	0.232	0.258	142.8	109.0	163.1	140.0
NGC 4278	E	0.83	20.2	0.136	0.119	0.138	0.100	18.8	8.7	16.8	26.6
NGC 4291	E	0.30	13.6	0.254	0.282	0.276	0.225	106.0	104.6	104.8	102.9
NGC 4365	E	1.21	47.3	0.292	0.300	0.256	0.281	44.5	45.1	42.4	40.7
NGC 4382	S0	0.27	11.1	0.416	0.506	0.264	0.221	43.2	43.2	30.7	27.9
NGC 4472	E ^d	1.21	48.8	0.129	0.133	0.169	0.181	161.0	160.3	159.1	157.7
NGC 4552	E ^d	0.38	29.7	0.181	0.145	0.064	0.095	136.3	132.3	124.7	131.4
NGC 4589	E	0.20	70.8	0.366	0.365	0.224	0.248	112.8	112.9	83.7	74.5
NGC 4649	E	2.51	62.8	0.053	0.050	0.204	0.218	93.6	91.2	101.8	104.1
NGC 5061	E	0.22	68.4	0.053	0.072	0.132	0.171	179.8	175.0	110.6	113.6
NGC 5419	E ^d	1.43	55.0	0.182	0.187	0.201	0.233	92.9	93.6	77.9	72.1
NGC 5557	E	0.23	30.2	0.050	0.067	0.156	0.180	87.9	79.4	95.7	88.8
NGC 5813	S0	0.35	7.1	0.321	0.452	0.100	0.099	134.9	140.4	148.1	139.1
NGC 5982	E	0.25	26.8	0.038	0.019	0.327	0.295	124.2	92.8	108.7	107.2
NGC 6849	SB0	0.18	7.8	0.056	0.061	0.367	0.344	8.4	163.5	24.0	23.2
NGC 7619	E	0.49	72.2	0.381	0.420	0.189	0.181	35.3	35.7	40.4	39.4

Notes.—Col. (1) Galaxy name. Col. (2) Morphological classification taken from Dullo & Graham (2014). The superscript *d* shows galaxies initially classified as ellipticals but which have recently been re-classified as disc galaxies in the literature by Laurikainen et al. (2010). Col. (3) Core-Sérsic break radius (Dullo & Graham 2014, their Table 2). Col. (4) The spheroid effective half light radius (Dullo & Graham 2014, their Table 2). Col. (5) PSF-affected ellipticity at the core-Sérsic break radius determined using our ELLIPSE fit data. Col. (6) The Lauer et al. (2005) PSF-deconvolved ellipticity at the core-Sérsic break radius R_b . Cols. (7) and (8) Average ellipticities measured using our ELLIPSE fit data over the intervals $R_e/2 < R < R_e$ and $R > R_e$, respectively. Col. (9) PSF-affected position angle at the core-Sérsic break radius. Col. (10) The Lauer et al. (2005) PSF-deconvolved position angle at R_b . Cols. (11) and (12) Average position angles over $R_e/2 < R < R_e$ and $R > R_e$, respectively. Position angles of the isophotes are measured from north to east.

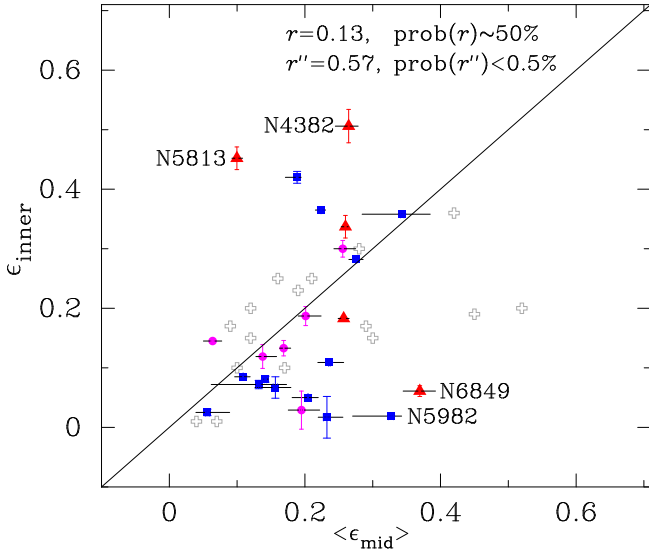


FIG. 3.— Top panel: ellipticity at the core-Sérsic break radius (ϵ_{inner}) versus the average ellipticity between $R_e/2$ and R_e ($\langle\epsilon_{\text{mid}}\rangle$). The solid one-to-one line is shown for comparison. The values r and $\text{prob}(r)$ are the Pearson correlation coefficient and the associated probability, respectively, while r'' and $\text{prob}(r'')$ are the Pearson coefficient and its probability after excluding three outliers (NGC 5813, NGC 5982 and NGC 6849). Solid horizontal lines connect the highest and lowest galaxy ellipticities between R_e and $R_e/2$. Open crosses represent “core” galaxies taken from Ryden et al. (2001, their Table 1), the remaining symbols are the same as in Fig. 1.

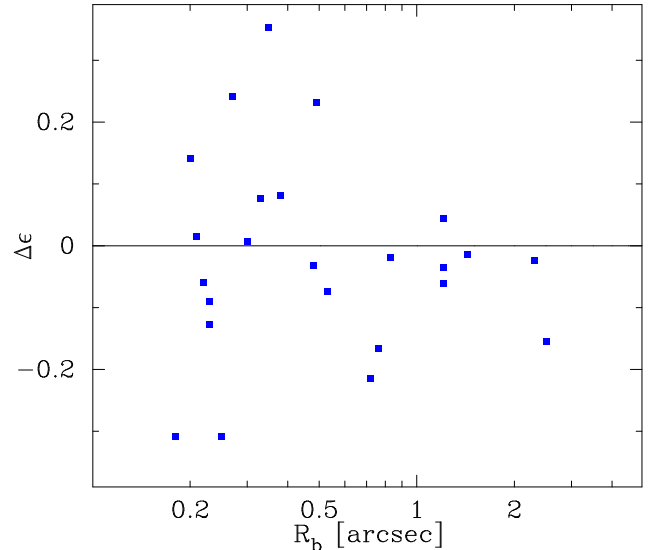


FIG. 4.— Residual of the relation between ϵ_{inner} and $\langle\epsilon_{\text{mid}}\rangle$ relative to the one-to-one line ($\Delta\epsilon = \epsilon_{\text{inner}} - \langle\epsilon_{\text{mid}}\rangle$, Fig. 3) against core-Sérsic break radius R_b . This reveals that the negative $\Delta\epsilon$ of galaxies are not because of the influence of seeing on smaller cores.

Our ellipticities, ϵ_{inner} and $\langle\epsilon_{\text{mid}}\rangle$, are broadly consistent with the results from previous works which showed that massive, luminous early-type galaxies, most of which are presumably core-Sérsic galaxies, tend to be rounder ($\epsilon \lesssim 0.25$) than their less luminous counterparts, i.e., the Sérsic galaxies, $\epsilon \gtrsim 0.25$ (e.g., Davies et al. 1983; Jaffe et al. 1994; Ferrarese et al. 1994; Faber et al. 1997;

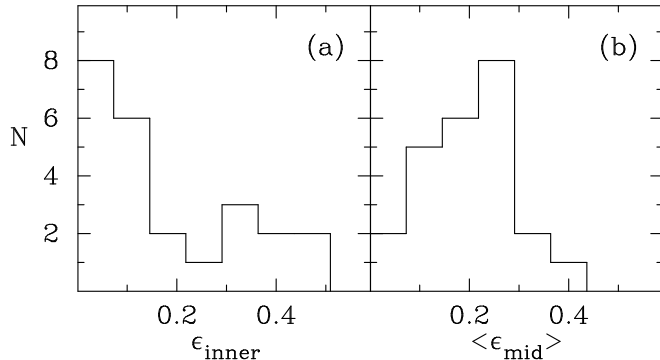


FIG. 5.— Inner and middle (radii) ellipticity distributions for our core-Sérsic galaxies (left and right, respectively).

Ryden et al. 2001; Alam & Ryden 2002; Vincent & Ryden 2005; Lauer et al. 2005; Ferrarese et al. 2006; Emsellem et al. 2007, 2011; Holden et al. 2009; Cappellari et al. 2011). Overall, our core-Sérsic galaxies have inner and outer ellipticity distributions with median ellipticities of $\epsilon_{\text{med}} = 0.13 \pm 0.01$, and $\epsilon_{\text{med}} = 0.20 \pm 0.01$, respectively (Fig. 5). These ellipticities remain the same after excluding the three previously mentioned outliers. This tendency for core-Sérsic galaxies to have ϵ_{inner} rounder than $\langle \epsilon_{\text{mid}} \rangle$ (Fig. 5) may reflect the influence of the central supermassive black hole at these galaxies’ core regions. However, this does not necessarily imply a trend between $\epsilon_{\text{inner}} - \langle \epsilon_{\text{mid}} \rangle$ (or $\epsilon_{\text{inner}} / \langle \epsilon_{\text{mid}} \rangle$) and the supermassive black hole mass M_{BH} (or mass deficit-to-black hole mass ratio, $M_{\text{def}}/M_{\text{BH}}$, Section 3.3). The quoted errors associated with the median values of ϵ_{inner} and $\langle \epsilon_{\text{mid}} \rangle$ above are the uncertainties on the median, and not the 1σ scatter. These errors agree with those quoted by Holden et al. (2009, their Section 3.3).

3.3. $M_{\text{def}}/M_{\text{BH}}$

In Fig. 6, open circles represent the ratios of stellar mass deficit to black hole mass, $M_{\text{def}}/M_{\text{BH}}$ ($\approx 0.5 N$, where N is the number of “dry” major mergers, Merritt 2006) taken from Dullo & Graham (2014, their Table 4). The sizes of these circles increase with increasing $M_{\text{def}}/M_{\text{BH}}$ ratio. The ellipticity distribution seen there suggests that galaxies which have experienced more mergers are rounder (i.e., ϵ_{inner} and $\langle \epsilon_{\text{mid}} \rangle \lesssim 0.2$). We use the two-sample Kolmogorov-Smirnov (KS) test and the Anderson-Darling (AD) test (Scholz & Stephens 1987) to quantify this difference in the ellipticity distribution between the (seven) galaxies with large $M_{\text{def}}/M_{\text{BH}}$ ratios (≥ 2.5) and the (17) galaxies with $M_{\text{def}}/M_{\text{BH}} < 2.5$. The results from these two tests agree very well. There is a $\sim 25\%$ probability that the inner ellipticity (ϵ_{inner}) distributions of galaxies with $M_{\text{def}}/M_{\text{BH}} \geq 2.5$ and $M_{\text{def}}/M_{\text{BH}} < 2.5$ are drawn from the same distribution, while for the mid-radii ellipticity ($\langle \epsilon_{\text{mid}} \rangle$), this probability decreases to $\sim 10\%$. Further, excluding the nucleated galaxy NGC 4365 (see Section 3.1)—which is the only galaxy with both high ellipticities (ϵ_{inner} and $\langle \epsilon_{\text{mid}} \rangle > 0.20$) and $M_{\text{def}}/M_{\text{BH}} \geq 2.5$ —the probabilities corresponding to the inner and mid radii ellipticities drop to $\sim 9\%$ and $\sim 2.5\%$, respectively. Although the two-dimensional KS test (Peacock 1983; Fasano & Franceschini 1987) is recommended for sample sizes ≥ 10 , we perform this test (including NGC 4365) and find a 3.2% probability that the ellipticities (ϵ_{inner} , $\langle \epsilon_{\text{mid}} \rangle$) of galax-

ies with $M_{\text{def}}/M_{\text{BH}} \geq 2.5$ and $M_{\text{def}}/M_{\text{BH}} < 2.5$ are sampled from the same distribution. Excluding NGC 4365, this drops to 0.3%.

We have additionally checked and found that this trend between the galaxy isophotal shape and the $M_{\text{def}}/M_{\text{BH}}$ ratio is not simply because more luminous galaxies are rounder. For our core-Sérsic galaxies, there is no obvious trend between the absolute magnitude (Dullo & Graham 2014, their Table 1) and the ellipticity (Fig. 7, see also Lauer et al. 2005, their Fig. 6). The Pearson correlation coefficient for the $\epsilon_{\text{inner}} - M_V$ relation (Fig. 7) is $r \approx 0.24$ with the corresponding probability $P(r) \approx 24\%$.

4. POSITION ANGLES

In this section we evaluate the robustness of our position angle (P.A.) measurements, and compare the inner and outer orientations (Figs. 8 and 9). In order to check on the effect of the PSF, in Fig. 8a we compare the PSF-affected position angles from our ELLIPSE fits with the Lauer et al. (2005) PSF-deconvolved position angle both determined at the core-Sérsic break radii. The position angles from these two works agree well except for four galaxies (NGC 0741, NGC 1016, NGC 3842 and NGC 5982), two of which are discussed below. The strong correlation between the average P.A.s which are determined over the radial intervals $R_e/2 < R < R_e$ and $R_e < R \lesssim 100''$ (Fig 8b) implies that the orientations of the galaxies remain, on average, unchanged between $R_e/2$ and $R \approx 100''$.

Using the PSF-deconvolved P.A. profile (Lauer et al. 2005), we find that about half of the galaxies in our sample show isophotal twist higher than 10° inside their cores, i.e., $R < R_b$, (Fig 9, vertical solid lines). At mid radii ($R_e/2 < R < R_e$) the galaxies display modest ($\sim 5^\circ$) to no twist (Fig 9, horizontal solid lines). Lauer et al. (2005, their Fig. 9) carried out detailed analyses of isophotal twists for their “core” and “power-law” galaxies⁵ and also concluded that the amplitude of twists are larger at small radii. This result also holds for our “clean” sample of galaxies with partially depleted cores relative to their outer Sérsic profile, having also removed galaxies with additional nuclear stellar components.

Also evident in Fig. 9, is that despite the twists, the galaxies’ orientations at their break radii are fairly aligned with the spheroid’s outer orientation except for five galaxies (NGC 0741, NGC 3842, NGC 4589, NGC 5061 and NGC 6849) with inner position angles which are twisted by $\gtrsim 27^\circ$ from the outer position angle.

NGC 0741, NGC 3842 and NGC 6849 show strong isophotal twists at their break radii coincident with local minima in their ellipticities, but for NGC 5061 the strong 30° twist and the ellipticity minimum which occurs between $3''$ and $10''$ may be a result of tidal effects (Tal et al. 2009). While the correlation between high twist amplitudes and low isophote ellipticities has already been known for some time (e.g., Galleta 1980; Nieto et al. 1992; Rahman & Shandarin 2004), these four galaxies have interesting features discussed in the literature. NGC 0741 is a nucleated galaxy (e.g., Dullo &

⁵ We refer to “power-law” galaxies as “Sérsic” galaxies because their spheroids’ light profiles are well described by the curved Sérsic model rather than by a straight power-law (e.g., Trujillo et al. 2004).

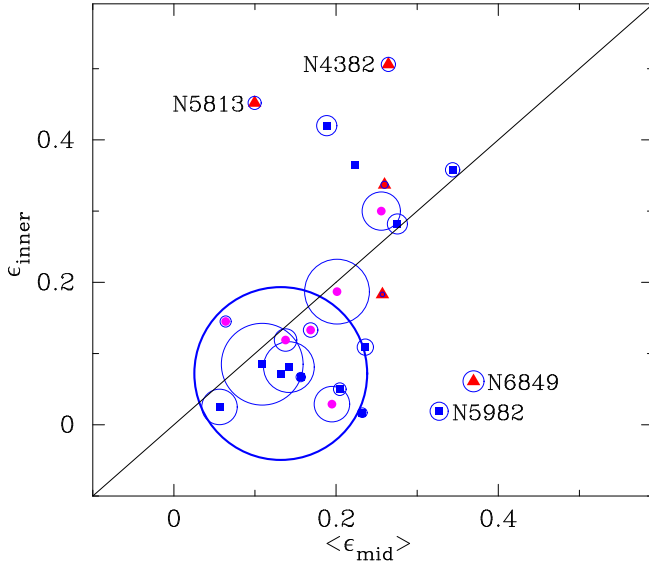


FIG. 6.— Similar to Fig. 3, circles designate the (stellar mass deficit)-to-(black hole mass) ratios. The sizes of these circles increase when the (mass deficit)-to-(black hole mass) ratio increases. Symbols are as in Fig. 1.

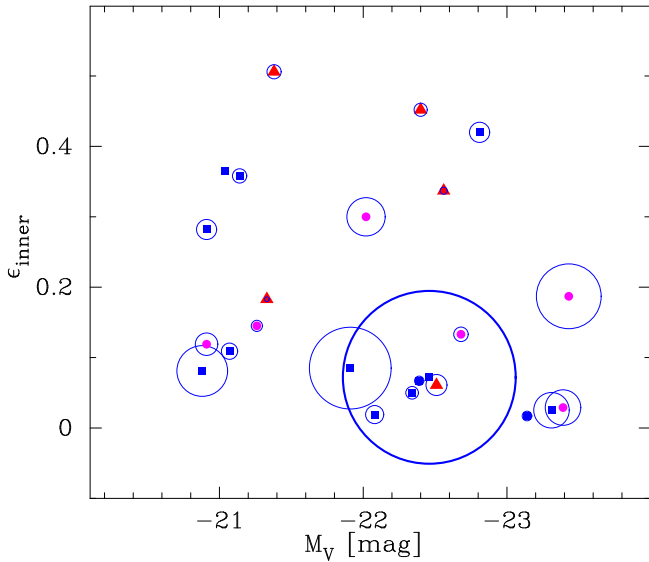


FIG. 7.— Similar to Fig. 6, but now comparing the inner ellipticity (ϵ_{inner}) and the spheroidal absolute magnitude (M_V ; Dullo & Graham 2014, their Table 1).

Graham 2012), NGC 3842 is a bright cluster galaxy that has an ultramassive black hole ($M_{\text{BH}} = 9.7 \times 10^9 M_{\odot}$) with a $1''.2$ radius of influence (McConnell et al. 2011) whereas the S0 galaxy NGC 6849 has an inner bar which manifests as a peak in the ellipticity profile (see Dullo & Graham 2013). The elliptical galaxy NGC 5061 has the largest Sérsic index and the biggest $M_{\text{def}}/M_{\text{BH}}$ ratio from the Dullo & Graham (2014) sample, also, Tal et al. (2009) identified a prominent tidal tail associated with this galaxy. The remaining outlier in the $\text{P.A.}_{\text{inner}} - \langle \text{P.A.}_{\text{mid}} \rangle$ diagram, NGC 4589 with a dust lane in the inner regions, $R \lesssim 10''$, (e.g., Möllenhoff & Bender 1989; Tomita et al. 2000), has isophotes which smoothly rotate from $\text{P.A.} \sim 112^\circ$ at $R_b \sim 0.2''$ to $\text{P.A.} \sim 85^\circ$ at $R_e \sim 71''$. This dust lane is visible in the optical *HST*/WFPC2

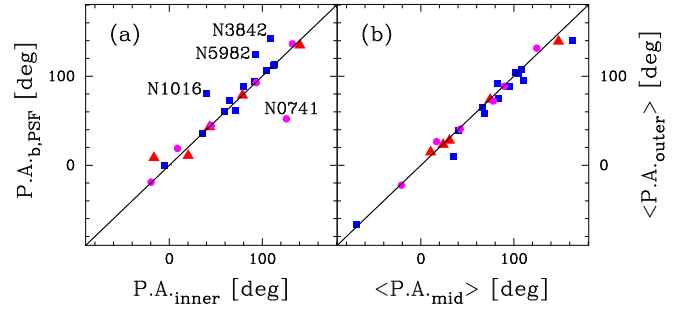


FIG. 8.— Panel (a): comparison of our PSF-affected position angle at the core-Sérsic break radius ($\text{P.A.}_{\text{b,PSF}}$) and the position angle at the core-Sérsic break radius ($\text{P.A.}_{\text{inner}}$) from the PSF-deconvolved profile of Lauer et al. (2005). Panel (b): average position angles measured at large radii $R > R_e$ ($\langle \text{P.A.}_{\text{outer}} \rangle$) versus average ellipticity measured between $R_e/2$ and R_e ($\langle \text{P.A.}_{\text{mid}} \rangle$). Symbols are as in Fig. 1.

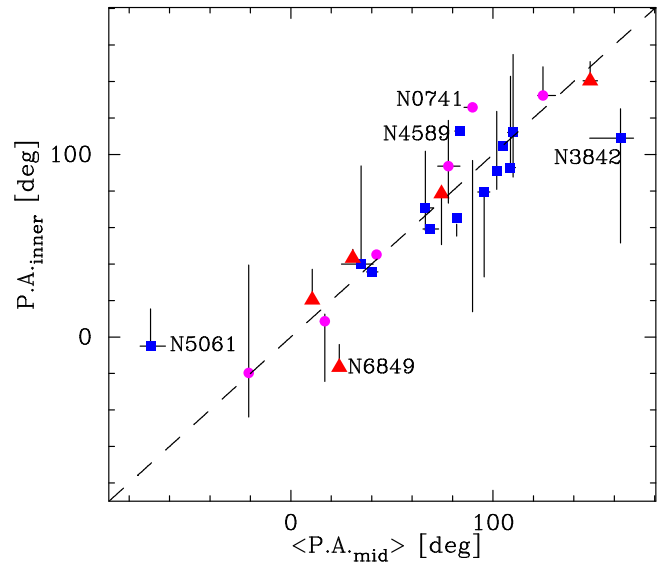


FIG. 9.— Position angle measured at our core-Sérsic break radius ($\text{P.A.}_{\text{inner}}$) versus the average position angle determined between $R_e/2$ and R_e ($\langle \text{P.A.}_{\text{mid}} \rangle$). The vertical (horizontal) solid line connects two P.A.s which yield the highest isophotal twist inside the core (in the range $R_e/2 < R < R_e$). Symbols are as in Fig. 1.

F555W (*V*-band) image.

5. CORE-SÉRSIC GALAXY FORMATION, SHAPE AND ORIENTATION

Understanding the radial stellar light distributions, and the radial variation of the shapes and orientations of core-Sérsic galaxies (Sections 3 and 4) can potentially provide valuable clues to the details of the mechanisms which drive their formation and evolution. On the theoretical side, it has been shown that simulated “dry merger” remnants of spheroids (or bulge-dominated systems) mimic the slowly rotating massive galaxies with low ellipticities (e.g., Khochfar & Burkert 2003; Boylan-Kolchin et al. 2006; Naab et al. 2006; Naab et al. 2007; Burkert et al. 2008; Hopkins et al. 2009). The final shape of a merger remnant depends on the mass ratio and gas fraction of the progenitors (e.g., Negroponte & White 1983; Barnes 1988; Hernquist 1992; Naab & Burkert 2003; Bournaud, Jog & Combes 2005; Jesseit, Naab & Burkert 2005; Naab & Trujillo 2006). Slowly rotating, round core-Sérsic galaxies are preferentially gener-

ated through collisionless (gas-poor) 1:1 mergers or generations of re-mergers (e.g., Naab et al. 2007; Burkert et al. 2008; Krajnović et al. 2013). The Hopkins et al. (2009) simulations argued that the low ellipticities of massive galaxies are recovered only if the initial progenitor spheroids are created from gas-rich (dissipative) mergers (see also Naab et al. 2013).

N-body simulations have shown that dissipationless major mergers of galaxies involving supermassive black holes naturally generate remnants which resemble core-Sérsic elliptical galaxies (e.g., Ebisuzaki et al. 1991; Milosavljević & Merritt 2001; Merritt 2006). Since it is predominantly stars on sufficiently radial orbits that pass close to a coalescing black hole binary and then get ejected, this causes the deficit of radial orbits and a dominance of tangential orbits inside R_b (e.g., Quinlan & Hernquist 1997; Milosavljević & Merritt 2001; Gebhardt et al. 2003; Thomas et al. 2014). Assuming that this scattering process ejects stars on radial orbits of all orientation, it suggests that the final isophotes within the galaxy core are likely to be round. In addition, many authors have pointed out the role of a single central supermassive black hole in shaping the innermost regions of triaxial galaxies, arguing that the disruption of box orbits passing too close to the black hole results in a nearly spherical (round) core (Merritt & Poon 2004). Indeed, as noted in Section 3.2, the median ellipticity of our core-Sérsic galaxies at the break radii (0.13 ± 0.01) tend to be more round than the median ellipticity at larger radii (0.20 ± 0.01), suggestive of i) stellar scattering by a binary supermassive black hole and/or ii) the influence of the central supermassive black hole after coalescence of the black hole binary.

The sizes and the stellar mass deficits of depleted galaxy cores scale with the mass of the central supermassive black hole (e.g., Graham 2004; Ferrarese et al. 2006; Lauer et al. 2007; Rusli et al. 2013; Dullo & Graham 2014). The formation of these cores is predicted to be a cumulative process, such that $M_{\text{def}} \approx NM_{\text{BH}}$ in individual galaxies, where N is the number of successive major “dry” mergers (Merritt 2006). In Dullo & Graham (2014) we measured central stellar mass deficits typically in the range $0.5 - 4 M_{\text{BH}}$ for the 24 core-Sérsic galaxies studied here. We found that $M_{\text{def}} \propto M_{\text{BH}}^{3.70 \pm 0.76}$ for the sample ensemble. Interestingly, as noted in Section 3.3 (Fig. 6), galaxies with larger (mass deficit)-to-(black hole mass) ratios possess round cores and round outer regions. Given the predicted relation between this $M_{\text{def}}/M_{\text{BH}}$ ratio and the number of major mergers (Merritt 2006), this result suggests that galaxies which have experienced multiple dissipationless mergers are round.

This new observation is in good agreement with the simulations by Weil & Hernquist (1996). Further, Kuehn & Ryden (2005, their Figs. 6 and 7) showed that galaxies in high density environment tend to be round. Hao et al. (2006) also arrived at similar conclusions regarding the relation between the ellipticities of early-type galaxies and their local density. Likewise, Ryden et al. (2001) studied the relation between galaxy shape and age while Vincent & Ryden (2005, see also Alam & Ryden 2002) examined the dependence of galaxy shapes on the luminosities. These studies concluded that brighter galaxies with old stellar populations, such as the core-Sérsic galax-

ies, are rounder than their fainter counterparts which have young stellar populations (see also, e.g., Lauer et al. 2005; Ferrarese et al. 2006). Most recently, Weijmans et al. (2014) argued that slow rotating early-type galaxies tend to be rounder than fast rotating galaxies (see also Emsellem et al. 2007, 2011; Cappellari et al. 2011) which contain discs. Here we went one step further and showed for the first time a tendency (albeit only 2 σ significance) for galaxies with large $M_{\text{def}}/M_{\text{BH}}$ ratios to have round cores ($\epsilon_{\text{inner}} \lesssim 0.2$), while other galaxies with $M_{\text{def}}/M_{\text{BH}} < 2.5$ can have more elliptically-shaped cores ($\epsilon_{\text{inner}} > 0.2 - 0.4$) in addition to roundish cores. Using the two-dimensional KS test, we find that the probabilities that galaxies with $M_{\text{def}}/M_{\text{BH}} \geq 2.5$ and $M_{\text{def}}/M_{\text{BH}} < 2.5$ are drawn from the same parent population is 3.2%. Note that this (weak) trend between the galaxy ellipticity and the $M_{\text{def}}/M_{\text{BH}}$ ratio is not simply because brighter galaxies are rounder (see Section 3.3).

In Figs. 3 (and 9) we have illustrated a fair agreement between the break ellipticities ϵ_{inner} (and position angles $\langle \text{P.A.}_{\text{inner}} \rangle$) and the mid-radii ellipticities $\langle \epsilon_{\text{mid}} \rangle$ (and position angles $\langle \text{P.A.}_{\text{mid}} \rangle$) for our core-Sérsic galaxies. This result is consistent with the notion that core-Sérsic galaxies are formed through major “dry” mergers involving supermassive black holes. That is, the violent dissipationless relaxation and phase mixing of progenitor stars (e.g., Naab et al. 2006; Burkert et al. 2008; Hopkins et al. 2009) together with the chaotic (and possibly isotropic) stellar scattering by the central supermassive black hole (e.g., Norman, May, & van Albada 1985; Gerhard & Binney 1985) create a round core-Sérsic spheroid with similarly aligned and shaped inner and outer regions. Indeed, the bulk (75%) of our core-Sérsic galaxies have values for ϵ_{inner} and $\langle \epsilon_{\text{mid}} \rangle$ which are smaller than 0.30 (Fig 5).

In general, Figs. 3 and 9 agree with the works by Hao et al. (2006) and Chaware et al. (2014). Hao et al. (2006) reported differences in the ellipticity and position angle between 1 and 1.5 Petrosian half-light radii for nearby early-type galaxies more elliptical than $\epsilon = 0.3$. However, these differences in the ellipticity and position angle were statistically less significant for the rounder galaxies with $\epsilon < 0.3$ and may have been associated with the increasing dominance of a disk at large radii. Chaware et al. (2014) found good agreement between the isophotal shapes and orientations of the inner (seeing radius to 1.5 Petrosian half-light radius) and intermediate (1.5 Petrosian half-light radius to 3.0 Petrosian half-light radius) regions of 132 distant ($0.1 < z < 0.3$) early-type galaxies, most of which have $-17 < M_B < -21$ mag. However, they reported that these galaxies’ shapes and orientations tend, on average, to change as one goes from intermediate to larger radii. They concluded that this may be because of the inclusion of galaxies that are still unrelaxed. Thus, the good agreement between the inner and outer ellipticities and position angles that we find here for our sample of nearby core-Sérsic galaxies with $M_V \lesssim -20.7$ mag (Figs. 3 and 9) is generally consistent with the results of Hao et al. (2006) and Chaware et al. (2014).

6. CONCLUSIONS

We have used the IRAF ELLIPSE task to extract the radial ellipticity and position angle profiles for a sample of 24 nearby core-Sérsic galaxies observed with the *HST*

WFPC2 and ACS cameras. We additionally used the inner ($R \lesssim 3''$) PSF-deconvolved ellipticity and position angle profiles from Lauer et al. (2005) to account for the *HST* PSF. We found that the PSF did not appear to heavily affect the ellipticities and position angles at the break radii of our core-Sérsic galaxies (Figs. 1a, 4 and 8). We explored the radial variation of the galaxies' shapes and orientations. Our principal conclusions are:

1. For the bulk of the core-Sérsic galaxies, we measured ellipticities and position angles at the core-Sérsic break radii that are in fair agreement with the average mid-radii ellipticities and position angles determined over $R_e/2 < R < R_e$ (Figs. 3, 9).

2. The median inner ellipticity for our sample is $\epsilon_{\text{med}} = 0.13 \pm 0.01$, rounder than the median ellipticity for the outer regions $\epsilon_{\text{med}} = 0.20 \pm 0.01$. 13 of our 24 galaxies have inner ellipticities (ϵ_{inner}) which are smaller than the mid-radii ellipticities ($\langle \epsilon_{\text{mid}} \rangle$), while for 4/24 galaxies ϵ_{inner} and $\langle \epsilon_{\text{mid}} \rangle$ are consistent. The remaining 7/24 galaxies have values for ϵ_{inner} which are greater

than $\langle \epsilon_{\text{mid}} \rangle$ (Figs. 3, 5). This overall trend may indicate the influence of the central supermassive black hole in the inner regions of the galaxies.

3. Core-Sérsic galaxies with larger (stellar mass deficit)-to-(SMBH mass), $M_{\text{def}}/M_{\text{BH}}$ ratios typically have quite round isophotes, suggesting a possible link between the shapes of the galaxies and their merger histories. Excluding the only galaxy with an apparent elongated nuclear star cluster, the probability that the ellipticity distributions of galaxies with $M_{\text{def}}/M_{\text{BH}} \geq 2.5$ and $M_{\text{def}}/M_{\text{BH}} < 2.5$ are drawn from the same distribution drops from 3.2% to 0.3% (Section 3.3).

7. ACKNOWLEDGMENTS

This research was supported under the Australian Research Council's funding scheme (DP110103509 and FT110100263). We are grateful to Paolo Bonfini for providing the GALFIT ellipticities and position angles.

REFERENCES

- Alam, S. M. K., & Ryden, B. S. 2002, *ApJ*, 570, 610
 Barnes J. E., 1988, *ApJ*, 331, 699
 Barnes J. E., 1998, in Kennicutt R. C., Jr, Schweizer F., Barnes J. E., Friedli D., Martinet L., Pfenniger D., eds, *Saas-Fee Advanced Course 26: Galaxies: Interactions and Induced Star Formation Dynamics of Galaxy Interactions*. Springer-Verlag, Berlin, p. 275
 Begelman, M. C., Blandford, R. D., & Rees, M. J. 1980, *Nature*, 287, 307
 Bender, R., Döbereiner, S., Möllenhoff, C. 1988, *A&AS*, 74, 385
 Binney, J. 1978, *MNRAS*, 183, 501
 Bonfini, P., 2014, *PASP*, accepted
 Bournaud, F., Jog, C. J., & Combes, F. 2005, *A&A*, 437, 69
 Boylan-Kolchin, M., Ma, C.-P., & Quataert, E. 2006, *MNRAS*, 369, 1081
 Burkert A., Naab T., Johansson P. H., Jesseit R., 2008, *ApJ*, 685, 897
 Capaccioli M., Piotto G., Rampazzo R., 1988, *AJ*, 96, 487
 Cappellari M., et al., 2011, *MNRAS*, 416, 1680
 Carter D., 1987, *ApJ*, 312, 514
 Carlberg, R., Hartwick, F. D. A. 2014, *ApJ*, 789, 11
 Carollo, C. M., Franx, M., Illingworth, G. D., & Forbes, D. A. 1997, *ApJ*, 481, 710
 Chaware, L., et al., 2014, *ApJ*, 787, 102
 Côté, P., et al. 2006, *ApJS*, 165, 57
 Côté, P., et al. 2007, *ApJ*, 671, 1456
 Davies R. L., Efstathiou G., Fall S. M., Illingworth G., Schechter P. L., 1983, *ApJ*, 266, 41
 di Tullio G., 1979, *A&AS*, 37, 591
 Dullo, B. T., & Graham, A. W. 2012, *ApJ*, 755, 163
 Dullo, B. T., & Graham, A. W. 2013, *ApJ*, 768, 36
 Dullo, B. T., & Graham, A. W. 2014, arXiv:1310.5867, in press
 Ebisuzaki, T., Makino, J., & Okumura, S. K. 1991, *Natur*, 354, 212
 Emsellem E. et al., 2007, *MNRAS*, 379, 401
 Emsellem E., et al., 2011, *MNRAS*, 414, 888
 Faber, S. M., Tremaine, S., Ajhar, E. A., et al. 1997, *AJ*, 114, 1771
 Fasano, G., & Franceschini, A. 1987, *MNRAS*, 225, 155
 Ferrarese L., van den Bosch F. C., Ford H. C., Jaffe W., OConnell R. W., 1994, *AJ*, 108, 1598
 Ferrarese L. et al., 2006, *ApJS*, 164, 334
 Floyd, D. J., Axon, D., Baum, S., et al. 2008, *ApJS*, 177, 148
 Gebhardt K. et al., 2003, *ApJ*, 583, 92
 Gerhard, O. E., & Binney, J. 1985, *MNRAS*, 216, 467
 Graham, A. W. 2004, *ApJL*, 613, L33
 Graham, A. W., Erwin, P., Trujillo, L., & Asensio Ramos, A. 2003, *AJ*, 125, 2951
 Hao, C.N., Mao, S., Deng, Z.G., Xia, X.Y., Wu, H. 2006, *MNRAS*, 370, 1339
 Hernquist, L., 1992, *ApJ*, 400, 460
 Hopkins P. F., Lauer T. R., Cox T. J., Hernquist L., Kormendy J., 2009, *ApJS*, 181, 486
 Holden, B. P., Franx, M., Illingworth, G. D., et al. 2009, *ApJ*, 693, 617
 Holley-Bockelmann K., Mihos J. C., Sigurdsson S., Hernquist L., Norman C., 2002, *ApJ*, 567, 817
 Hubble E. P., 1926, *ApJ*, 64, 321
 Jedrzejewski R., 1987, *MNRAS*, 226, 747
 Jedrzejewski R. I., Davies R. L., Illingworth G. D., 1987, *AJ*, 94, 1508
 Kauffmann G., White S. D. M., Guiderdoni B., 1993, *MNRAS*, 264, 201
 Kent S. M., 1984, *ApJS*, 56, 105
 Krajnović, D., Karick, A. M., Davies, R. L., et al. 2013, *MNRAS*, 433, 2812
 Lambas D., Maddox S., Loveday J., 1992, *MNRAS*, 258, 404
 Lauer, T. R. et al. 2005, *AJ*, 129, 2138
 Lauer T. R. et al., 2007, *ApJ*, 662, 808
 Laurikainen E., Salo H., Buta R., Knapen J. H., & Comerón S. 2010, *MNRAS*, 405, 1089
 Lena, D., et al., 2014, *ApJ*, arXiv:1409.3976
 McGlynn, T. A. 1984, *ApJ*, 281, 13
 McConnell, N. J., Ma, C.-P., Gebhardt, K., et al. 2011, *Nature*, 480, 215
 Merritt, D. 2000, in *ASP Conf. Ser. 197, Dynamics of Galaxies: from the Early Universe to the Present*, ed. F. Combes, G. A. Mamon, & V. Charmandaris (San Francisco: ASP), 221
 Merritt, D., 2006, *ApJ*, 648, 976
 Merritt D., Poon M. Y., 2004, *ApJ*, 606, 788
 Merritt, D., & Quinlan, G. 1998, *ApJ*, 498, 625
 Michard, R., Prugniel, P., 2004, *A&A*, 423, 833
 Milosavljević, M., & Merritt, D. 2001, *ApJ*, 563, 34
 Möllenhoff, C., & Bender, R. 1989, *A&A*, 214, 61
 Naab, T., & Burkert, A. 2003, *ApJ*, 597, 893
 Naab, T., Jesseit, R., Burkert, A., 2006, *MNRAS*, 372, 839
 Naab T., Johansson P. H., Ostriker J. P., Efstathiou G., 2007, *ApJ*, 658, 710
 Naab T., & Trujillo L., 2006, *MNRAS*, 369, 625
 Naab, T., Oser, L., Emsellem, E., et al. 2013, *MNRAS*, accepted (arXiv:1311.0284)
 Negroponte J., White S. D. M., 1983, *MNRAS*, 205, 1009
 Nieto, J.-P., & Bender, R. 1989, *A&A*, 215, 266
 Nieto, J.-L., Bender, R., Poulain, P., & Surma, P. 1992, *A&A*, 257, 97
 Norman, C. A., May, A., & van Albada, T. S. 1985, *ApJ*, 296, 20
 Peacock, J. A. 1983, *MNRAS*, 202, 615
 Peng C. Y., Ho L. C., Impey C. D., Rix H.-W., 2002, *AJ*, 124, 266
 Pichon, C., Pogosyan, D., Kimm, T., et al. 2011, *MNRAS*, 418, 2493
 Quinlan, G. D., & Hernquist, L. 1997, *NewA*, 2, 533
 Rahman N., Shandarin S. F., 2003, *MNRAS*, 343, 933
 Rahman N., Shandarin S. F., 2004, *MNRAS*, 354, 235

- Ravindranath, S., Ho, L. C., Peng, C. Y., Filippenko, A. V., & Sargent, W. L. W. 2001, *AJ*, 122, 653
- Rest, A., van den Bosch, F. C., Jaffe, W., et al. 2001, *AJ*, 121, 2431
- Rusli, S. P., Erwin, P., Saglia, R. P., et al. 2013, *AJ*, 146, 160
- Ryden B. S., Forbes D. A., Terlevich A. I., 2001, *MNRAS*, 326, 1141
- Scholz, F. W. & Stephens, M. A. 1987, *J. Amer. Stat. Assoc.*, 82, 918
- Schweizer, F. 1982, *ApJ*, 252, 455
- Tal, T., van Dokkum, P. G., Nelan, J., & Bezanson, R. 2009, *AJ*, 138, 1417
- Thomas, J., Saglia, R. P., Bender, R., Erwin, P., & Fabricius, M. 2014, *ApJ*, 782, 39
- Tomita, A., Aoki, K., Watanabe, M., Takata, T., & Ichikawa, S.-I. 2000, *AJ*, 120, 123
- Toomre, A., & Toomre, J. 1972, *ApJ*, 178, 623
- Trujillo I., Erwin P., Asensio Ramos A., & Graham A. W. 2004, *AJ*, 127, 1917
- van Albada T., 1982, *MNRAS*, 201, 939
- Vincent, R. A., & Ryden, B. S. 2005, *ApJ*, 623, 137
- Weijmans, A.-M., et al. 2014, *MNRAS*, arXiv:1408.1099
- Zaritsky, D. & Lo, K. Y. 1986, *ApJ*, 303, 66